Stem Cell Research 77 (2024) 103411

Contents lists available at ScienceDirect

Stem Cell Research

journal homepage: www.elsevier.com/locate/scr

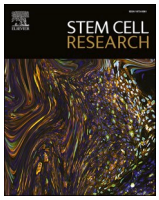

Lab Resource: Multiple Cell Lines

Generation of two iPSC lines from adult central core disease patients with dominant missense variants in the *RYR1* gene

Joshua S. Clayton [a,b,*], Christina Vo [a,b], Jordan Crane [a,b], Carolin K. Scriba [a,b,c], Safaa Saker [d], Thierry Larmonier [d], Edoardo Malfatti [e,f], Norma B. Romero [g,h], Gianina Ravenscroft [a,b], Nigel G. Laing [a,b], Rhonda L. Taylor [a,b]

[a] *Harry Perkins Institute of Medical Research, QEII Medical Centre, Nedlands, WA, Australia*
[b] *Centre for Medical Research, University of Western Australia, QEII Medical Centre, Nedlands, WA, Australia*
[c] *Neurogenetics Laboratory, Department of Diagnostic Genomics, PP Block, QEII Medical Centre, Nedlands, WA, Australia*
[d] *Genethon, DNA and Cell Bank, 91000 Evry, France*
[e] *APHP, Centre de Référence de Pathologie Neuromusculaire Nord-Est-Ile-de-France, Henri Mondor Hospital, France*
[f] *Université Paris Est, U955, INSERM, IMRB, F-94010 Créteil, France*
[g] *Sorbonne Université, Myology Institute, Neuromuscular Morphology Unit, Center for Research in Myology, GH Pitié-Salpêtrière, Paris, France*
[h] *Centre de Référence de Pathologie Neuromusculaire Paris-Est, GHU Pitié-Salpêtrière, Assistance Publique-Hôpitaux de Paris, Paris, France*

A B S T R A C T

RYR1 variants are a common cause of congenital myopathies, including multi-minicore disease (MmD) and central core disease (CCD). Here, we generated iPSC lines from two CCD patients with dominant *RYR1* missense variants that affect the transmembrane (pore) and SPRY3 protein domains (p.His4813Tyr and p.Asn1346Lys, respectively). Both lines had typical iPSC morphology, expressed canonical pluripotency markers, exhibited trilineage differentiation potential, and had normal karyotypes. Together with existing *RYR1* iPSC lines, these represent important tools to study and develop treatments for *RYR1*-related myopathies.

Resource Table:

Unique stem cell lines identifier	1. HPIi008-A 2. HPIi009-A
Alternative name(s) of stem cell lines	1. RYR1-4833-R7 (HPIi008-A) 2. RYR1-15377-R1B (HPIi009-A)
Institution	Harry Perkins Institute of Medical Research
Contact information of distributor	Dr. Joshua Clayton joshua.clayton@perkins.org.au
Type of cell lines	iPSC
Origin	Human
Additional origin info required *for human ESC or iPSC*	1. HPIi008-A: 29 years, female, Caucasian 2. HPIi009-A: 28 years, male, Caucasian
Cell Source	Lymphoblastoid cell line (LCL) immortalized with Epstein Barr Virus
Clonality	Clonal
Method of reprogramming	Sendai virus (CytoTune-iPS 2.0^{TM})
Genetic Modification	Yes
Type of Genetic Modification	1. Inherited variant (dominant, 5 other affected family members across 4 generations)

(*continued on next column*)

(*continued*)

Unique stem cell lines identifier	1. HPIi008-A 2. HPIi009-A
	2. Unknown (segregation information not available)
Evidence of the reprogramming transgene loss (including genomic copy if applicable)	RT-PCR to confirm clearance of Sendai virus
Associated disease	Central core disease of muscle; CCD (OMIM#117000)
Gene/locus	1. HPIi008-A: Ryanodine Receptor 1, Skeletal Muscle (*RYR1*), NM_000540.3: c.14437C > T (p.His4813Tyr) 2. HPIi009-A: Ryanodine Receptor 1, Skeletal Muscle (*RYR1*), NM_000540.3: c.4038C > A (p.Asn1346Lys)
Date archived/stock date	Cell line stocks archived at Harry Perkins Institute, November 2022
Cell line repository/bank	1. https://hpscreg.eu/cell-line/HPIi008-A 2. https://hpscreg.eu/cell-line/HPIi009-A

(*continued on next page*)

* Corresponding author at: Harry Perkins Institute of Medical Research, QEII Medical Centre, Nedlands, WA, Australia.
E-mail address: joshua.clayton@perkins.org.au (J.S. Clayton).

https://doi.org/10.1016/j.scr.2024.103411
Received 26 March 2024; Accepted 30 March 2024
Available online 31 March 2024
1873-5061/© 2024 The Authors. Published by Elsevier B.V. This is an open access article under the CC BY license (http://creativecommons.org/licenses/by/4.0/).

(*continued*)

Unique stem cell lines identifier	1. HPIi008-A 2. HPIi009-A
Ethical approval	Personnes (Est IV DC-2012–1693), and national consent forms for genetic testing, banking and research were signed by the patients or their legal guardian. The patient's LCLs were banked by Genethon; activity authorization No. AC-2018–3156, import/ export authorization No. IE-2018–994. The study was approved by the University of Western Australia's Human Research Ethics Committee (approval number: RA/4/20/1008).

1. Resource utility

These lines complement our other dominant *RYR1* iPSCs derived from patients with central core disease (CCD) and malignant hyperthermia. The two lines here possess variants in either the transmembrane (pore) or SPRY3 domain of RyR1. Collectively, these iPSC lines will provide novel models to study CCD in a human context.

2. Resource details

CCD is a congenital myopathy typically diagnosed by the presence of centrally-located cores in type 1 myofibres. Common clinical features include muscle weakness and hypotonia presenting during infancy, delayed motor development, and joint contractures (Lorenzon and Beam, 2000; Quinlivan et al., 2003). CCD has been linked to the gene encoding the skeletal muscle ryanodine receptor, *RYR1* (Monnier et al., 2001; Wu et al., 2006).

Here, we generated iPSC lines from two CCD patients with dominant *RYR1* variants. Patient 1 (HPIi008-A) was originally diagnosed with rigid spine syndrome, which was subsequently re-classified as CCD based on histology and genetic testing. The patient has a dominantly-inherited *RYR1* c.14437C>T (p.His4813Tyr) variant, for which there is one prior *de novo* report in a case of *RYR1*-related myopathy (Klein et al., 2012). This variant sits within the pore region of the RyR1 protein, which contains many CCD-causing variants (Treves et al., 2005; Wu et al., 2006). Based on ACMG guidelines this variant is pathogenic.

Patient 2 (HPIi009-A) presented with exercise intolerance, fatigability and myalgia. They could walk normally and did not show rhabdomyolysis. Muscle biopsy confirmed CCD. This patient carries a *RYR1* c.4038C>A (p.Asn1346Lys) variant within the SPRY3 protein domain (Samsó, 2017). This variant has been previously reported in a 29 year-old patient with multi-minicore disease and severe scoliosis (Wu et al., 2018). However, that case also possessed a c.13320delG (p.Gly4407-Valfs*34) frameshift variant on the same allele, and a c.10561G>A (p.Gly3521Ser) on the other *RYR1* allele. There are eight VUS reports in ClinVar. Based on ACMG guidelines the variant is a VUS. The variant does not sit in any of the traditional *RYR1* "hotspots" (Treves et al., 2005). As this patient contains an *RYR1* variant that may or may not be causative of disease this line may serve as a good test-case, or control for additional *RYR1* lines that we and others have generated (Driver et al., 2023; Zhang et al., 2020).

Patient iPSCs were reprogrammed from lymphoblastoid cell lines (LCLs) using the CytoTune^{TM}-iPS 2.0 Sendai reprogramming kit and characterized after 10 passages (Table 1). Both lines displayed typical iPSC morphology and no spontaneous differentiation (Fig. 1A). iPSCs stained uniformly for pluripotency markers SOX2, TRA-1–60, OCT4, and SSEA4 by immunofluorescence (Fig. 1C, Fig. S1A). Transcript abundance of four pluripotency markers were comparable to a well-characterized control iPSC line, SCTi003-A (Fig. 1B). iPSCs were free of Sendai virus by RT-PCR (Fig. 1D) and did not show any significant chromosomal copy number abnormalities by hPSC genetic analysis (Fig. S1B).

Both HPIi008-A and HPIi009-A demonstrated good mesoderm and ectoderm potential by qRT-PCR and immunofluorescence following directed differentiation (Fig. 1E, Fig. S1C). Endoderm differentiation potential was significantly lower for both lines compared to SCTi003-A by qRT-PCR (Fig. 1E). This was supported by the presence of many SOX17-negative cell clusters in endoderm cultures, in contrast to SCTi003-A which produced uniform SOX17-positive cultures (Fig. S1C). However, given the function and restricted expression of RyR1 in skeletal muscle (mesoderm), a lack of robust endoderm differentiation potential is unlikely to negatively impact the disease modelling potential of these lines.

HPIi008-A and HPIi009-A had normal karyotypes by G-banding (46, XX and 46,XY, respectively) (Fig. 1F). STR profiles matched parental cells used for reprogramming at all 22 tested loci (available with

Table 1
Characterization and validation.

Classification	Test	Result	Data
Morphology	Photography Bright field	At P11: Normal morphology	Fig. 1 panel A
Phenotype	Qualitative analysis (immunocytochemistry)	At P11: Positive for OCT4, SOX2, SSEA4, TRA-1-60	Fig. 1 panel C, Supplementary Fig. 1 panel A
	Quantitative analysis (qRT-PCR)	At P10: Expression of *OCT4*, *SOX2*, *NANOG*, *CRIPTO*	Fig. 1 panel B
Genotype	Karyotype (G-banding) and resolution	At P13: 46, XX (normal female karyotype) for HPIi008-A, or 46, XY (normal male karyotype) for HPIi009-A Banding Resolution: 400 bands per haploid set 15 metaphases counted, 5 analyzed for each	Fig. 1 panel F; hPSC genetic analysis (P10): Supplementary Fig. 1 panel B
Identity	STR analysis	At P10: Matched to parental LCLs at 22/22 STR loci	Available with authors
Mutation analysis	Sequencing	At P10: Heterozygous for *RYR1* c.14437C > T variant (HPIi008-A) or *RYR1* c.4038C > A variant (HPIi009-A)	Fig. 1 panel G
Microbiology and virology	Mycoplasma	At P13: Negative for mycoplasma by PCR	Mycoplasma: Supplementary Fig. 1 panel D
	Sendai virus (SeV)Epstein Barr virus (EBV)	At P10: Negative for SeV by RT-PCR At P10: Negative for EBV by PCR	SeV: Fig. 1 panel D EBV: Supplementary Fig. 1 panel E
Differentiation potential	Directed differentiation	At P14 (HPIi008-A) or P18 (HPIi009-A): Enrichment of *TBXT* and *TBX6* (mesoderm), *OTX2* and *PAX6* (ectoderm), and *SOX17* and *GATA4* (endoderm) by qRT-PCR. Enrichment of Brachyury (mesoderm), OTX2 (ectoderm) and SOX17 (endoderm) by immunocytochemistry	Fig. 1 panel E (qRT-PCR); Supplementary Fig. 1 panel C (immunofluorescence)
Donor screening (OPTIONAL)	HIV 1 + 2 Hepatitis B, Hepatitis C	Not performed	
Genotype additional info (OPTIONAL)	Blood group genotyping	Not performed	
	HLA tissue typing	Not performed	

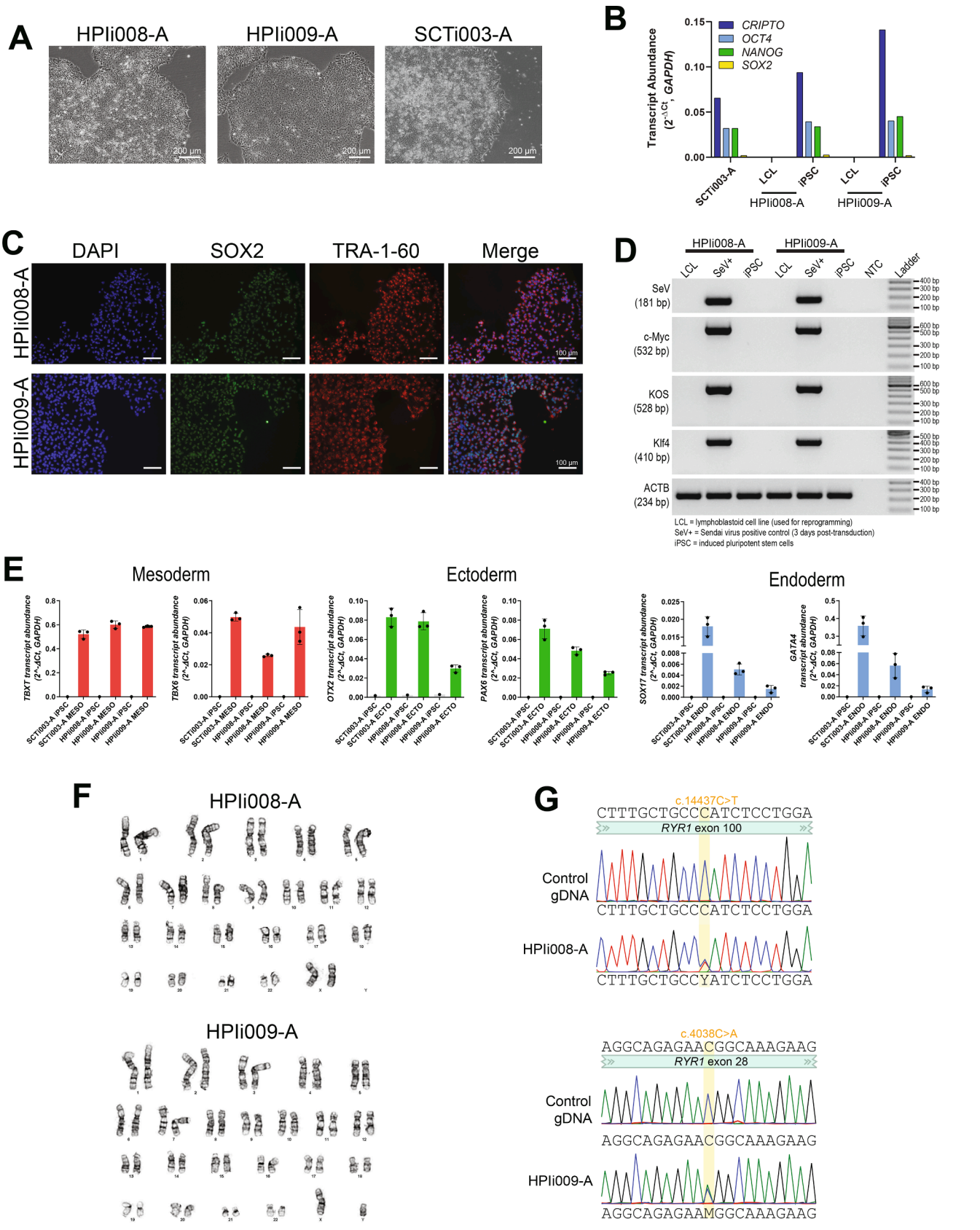

Fig. 1. Characterization of HPIi008-A and HPIi009-A iPSC lines.

authors). The expected *RYR1* variants were confirmed heterozygous in each line (Fig. 1G). Lines were also confirmed to be free of mycoplasma (Fig. S1D) and Epstein-Barr virus (Fig. S1E) by PCR.

3. Materials and methods

3.1. Reprogramming and maintenance of iPSC lines

Patient LCLs were cultured in RPMI-1640 medium supplemented with 10 % fetal bovine serum, 1 % L-glutamine, and 1 % penicillin–streptomycin (R10 medium). Reprogramming was performed with the CytoTune™-iPS 2.0 Sendai Reprogramming Kit (ThermoFisher) using 3 x 10^5 cells. Cells were plated on growth factor-reduced (GFR) Matrigel® (Corning; diluted 1:100 in DMEM/F12) and gradually transitioned from R10 to ReproTeSR™ (StemCell Technologies). Individual clones were picked and expanded in mTeSR™ Plus (StemCell Technologies) on GFR Matrigel. Following three rounds of manual picking, cells were routinely passaged with 1X Versene (ThermoFisher) at 1:12–1:20 with 10 μM ROCK inhibitor (Y-27632). Cells were cryopreserved in 90 % KnockOut™ Serum Replacement (ThermoFisher) with 10 % DMSO (Sigma). The control iPSC line SCTi003-A was purchased from StemCell Technologies and maintained as above. All cells were maintained at 37 °C and 5 % CO_2.

Table 2
Reagents details.

	Antibodies used for immunocytochemistry/flow-cytometry			
	Antibody	**Dilution**	**Company Cat #**	**RRID**
Pluripotency marker	Rabbit anti-OCT4	1:200	Thermo Fisher Cat# A24867	AB_2650999
Pluripotency marker	Mouse anti-SSEA4	1:100	Thermo Fisher Cat# A24866	AB_2651001
Pluripotency marker	Rat anti-SOX2	1:100	Thermo Fisher Cat# A24759	AB_2651000
Pluripotency marker	Mouse anti-TRA-1–60	1:100	Thermo Fisher Cat# A24868	AB_2651002
Secondary antibody	Alexa Fluor™ 594 donkey anti-rabbit	1:250	Thermo Fisher Cat# A21207	AB_141637
Secondary antibody	Alexa Fluor™ 488 goat anti-mouse IgG3	1:250	Thermo Fisher Cat# A24877	AB_2651008
Secondary antibody	Alexa Fluor™ 488 donkey anti-rat	1:250	Thermo Fisher Cat# A24876	AB_2651007
Secondary antibody	Alexa Fluor™ 594 goat anti-mouse IgM	1:250	Thermo Fisher Cat# A21044	AB_2535713
Differentiation marker (ectoderm)	Anti-human Otx-2 NL557-conjugated goat IgG	1:10	R&D systems Cat# SC022, Part# 967,389	AB_2889887
Differentiation marker (mesoderm)	Anti-human Brachyury NL557-conjugated goat IgG	1:10	R&D systems Cat# SC022, Part# 967,388	AB_2889887
Differentiation marker (endoderm)	Anti-human SOX17 NL637-conjugated goat IgG	1:10	R&D systems Cat# SC022, Part# 967,393	AB_2889887

	Primers		
	Target	**Size of band**	**Forward/Reverse primer (5′-3′)**
Pluripotency markers (qPCR)	*OCT4*	63 bp	F: GGGTTTTTGGGATTAAGTTCTTCA/ R: GCCCCCACCCTTTGTGTT
	SOX2	63 bp	F: CAAAAATGGCCATGCAGGTT/ R: AGTTGGGATCGAACAAAAGCTATT
	NANOG	111 bp	F: ACAACTGGCCGAAGAATAGCA/ R: GGTTCCCAGTCGGGTTCAC
	CRIPTO	66 bp	F: CGGAACTGTGAGCACGATGT/ R: GGGCAGCCAGGTGTCATG
Mesoderm markers (qPCR)	*TBXT*	109 bp	F: GGTCCAGCCTTGGAATGCCT/ R: CCGTTGCTCACAGACCACAG
	BMP4	135 bp	F: GCACTGGTCTTGAGTATCCTG/ R: TGCTGAGGTTAAAGAGGAAACG
Endoderm markers (qPCR)	*SOX17*	102 bp	F: GTGGACCGCACGGAATTTGA/ R: GCTGTCGGGGAGATTCACAC
	GATA4	100 bp	F: CAGCGAGGAGATGCGTCC/ R: AGACATCGCACTGACTGAGAA
Ectoderm markers (qPCR)	*OTX2*	106 bp	F: GACCCGGTACCCAGACATCTT/ R: GCGGCACTTAGCTCTTCGATT
	PAX6	120 bp	F: AACGATAACATACCAAGCGTGT/ R: GGTCTGCCCGTTCAACATC
House-keeping Genes (qPCR)	*GAPDH*	148 bp	F: TCGGAGTCAACGGATTTGGT/ R: TTGCCATGGGTGGAATCATA
Sendai virus vectors (RT-PCR)	Sendai virus (SeV) genome	181 bp	F: GGATCACTAGGTGATATCGAGC/ R: ACCAGACAAGAGTTTAAGAGATATGTATC
	KOS transgene	528 bp	F: ATGCACCGCTACGACGTGAGCGC/ R: ACCTTGACAATCCTGATGTGG
	Klf4 transgene	410 bp	F: TTCCTGCATGCCAGAGGAGCCC/ R: AATGTATCGAAGGTGCTCAA
	c-Myc transgene	532 bp	F: TAACTGACTAGCAGGCTTGTCG/ R: TCCACATACAGTCCTGGATGATGATG
House-keeping genes (RT-PCR)	*ACTB*	234 bp	F: GGACTTCGAGCAAGAGATGG/ R: AGCACTGTGTTGGCGTACAG
EBNA testing (PCR)	*BZLF-1*	637 bp	F: CACCTCAACCTGGAGACAAT/ R: TGAAGCAGGCGTGGTTTCAA
	LMP1	617 bp	F: ATGGAACACGACCTTGAGA/ R: TGAGCAGGATGAGGTCTAGG
	OriP	544 bp	F: TCGGGGGTGTTAGAGACAAC/ R: TTCCACGAGGGTAGTGAACC
House-keeping Genes (PCR)	*GAPDH*	452 bp	F: ACCACAGTCCATGCCATCAC/ R: TCCACCACCCTGTTGCTGTA
Targeted mutation analysis (PCR/sequencing) – HPIi008-A	*RYR1* (F primer used for Sanger sequencing)	375 bp	F: CTTCTCACCCGGAATGCCCTGATC R: TTATCCCTTCACCACCCACTGCCAC
Targeted mutation analysis (PCR/sequencing) – HPIi009-A	*RYR1* (F primer used for Sanger sequencing)	399 bp	F: CAGAACAGCCTGGTGGAGATGC R: AGGTTACTGTGGTTGCCTACTTGG

3.2. Trilineage differentiation

Directed differentiation was performed using the STEMdiff™ trilineage differentiation kit (StemCell Technologies). Cell pellets were collected using 1X TrypLE Express (Gibco).

3.3. Immunocytochemistry

Cells were fixed in 4 % paraformaldehyde for 15 min at room temperature (RT) and washed three times in 1X DPBS. Pluripotency staining was performed using the PSC 4-marker Immunocytochemistry Kit (Thermo Fisher). Germ layer staining was carried out per the Human Three Germ Layer 3-Color Immunocytochemistry Kit (SC022, R&D Systems). All primary antibody staining was performed overnight at 4 °C. Nuclei were stained with NucBlue™ Fixed Cell Stain for 10 min at RT (ThermoFisher). Samples were imaged on an Olympus IX71 with DP74 camera and CellSens software, or a CellInsight CX7 (SOX17 only due to NL637 conjugation).

3.4. DNA and RNA extraction

Genomic DNA was extracted using the QIAamp DNA Mini Kit (Qiagen). RNA was extracted using the RNeasy Mini Kit (Qiagen) and cDNA synthesized using the SuperScript™ III First-Strand Synthesis System (ThermoFisher).

3.5. Polymerase chain reaction (PCR)

Standard PCRs were performed using GoTaq® G2 Hot Start Mastermix (Promega) and a C1000 thermocycler (Bio-Rad). Cycling conditions for EBV and SeV detection: 95 °C/2 min, (95 °C/30 s, 60 °C/30 s and 72 °C/40 s) x 35, 72 °C/5 min; *RYR1* variant confirmation: 95 °C/5 min, (95 °C/30 s, 65 °C/30 s −0.5 °C/cycle, 72 °C/30 s) x 15, (98 °C/30 s, 57 °C/30 s, 72 °C/30 s) x 30, 72 °C/5 min. Primers are listed in Table 2.

3.6. Quantitative PCR (qRT-PCR)

qRT-PCRs were performed using the Rotor-Gene SYBR Green RT-PCR Kit (Qiagen) on a Rotor-Gene Q thermocycler using the following cycling conditions: 95 °C/5 min, (95 °C/10 s, 60 °C/15 s) x 45 cycles, followed by melt curve analysis. Data were normalized to *GAPDH* using the ΔC_T method. Primers are listed in Table 2.

3.7. Sanger sequencing

PCR products were purified using the MinElute PCR Purification Kit (Qiagen). Sanger sequencing was done by the Australian Genome Research Facility (Perth, WA, Australia).

3.8. Mycoplasma testing

All lines were screened for mycoplasma using the ATCC Universal Mycoplasma Contamination Kit.

3.9. Karyotyping

iPSCs were screened for common karyotypic abnormalities using the hPSC Genetic Analysis Kit (StemCell Technologies) on a Bio-Rad CFX. G-banding was performed by PathWest Diagnostic Genomics (Perth, WA, Australia).

3.10. Short tandem repeat (STR) typing

STR typing was performed at PathWest Diagnostic Genomics (Perth, WA, Australia) using the QSTR Plus assay (Elucigene).

3.11. Graphs and statistics

Graphs and statistics were done using GraphPad Prism 9.1.2.

CRediT authorship contribution statement

Joshua S. Clayton: Conceptualization, Data curation, Formal analysis, Funding acquisition, Investigation, Methodology, Project administration, Supervision, Writing – original draft. **Christina Vo:** Data curation, Formal analysis. **Jordan Crane:** Data curation, Formal analysis. **Carolin K. Scriba:** Data curation, Formal analysis. **Safaa Saker:** Resources. **Thierry Larmonier:** Resources. **Edoardo Malfatti:** Data curation, Formal analysis, Investigation, Resources. **Norma B. Romero:** Data curation, Formal analysis, Project administration, Resources. **Gianina Ravenscroft:** Funding acquisition, Supervision, Writing – review & editing. **Nigel G. Laing:** Funding acquisition, Supervision, Writing – review & editing. **Rhonda L. Taylor:** Conceptualization, Data curation, Formal analysis, Funding acquisition, Project administration, Supervision, Writing – review & editing.

Declaration of competing interest

The authors declare the following financial interests/personal relationships which may be considered as potential competing interests: Rhonda Taylor reports financial support was provided by Stan Perron Charitable Foundation.

Data availability

Data will be made available on request.

Acknowledgements

This work was supported by funding from the Stan Perron Charitable Foundation (202003010Research), awarded to Rhonda Taylor. We also gratefully acknowledge funding from the Australian National Health and Medical Research Council (NHMRC), including an EL2 Investigator Grant (APP2007769) to Gianina Ravenscroft. Rhonda Taylor is supported by a Raine Priming Grant (RPG54-21) from the Raine Medical Research Foundation. We also wish to gratefully acknowledge Dr Susan Treves for her intellectual input.

Appendix A. Supplementary data

Supplementary data to this article can be found online at https://doi.org/10.1016/j.scr.2024.103411.

References

Driver, K., Vo, C., Scriba, C.K., Saker, S., Larmonier, T., Malfatti, E., Romero, N.B., Ravenscroft, G., Laing, N.G., Taylor, R.L., Clayton, J.S., 2023. Generation of two induced pluripotent stem cell lines from a 33-year-old central core disease patient with a heterozygous dominant c.14145_14156delCTACTGGGACA (p.Asn4715_Asp4718del) deletion in the RYR1 gene. Stem Cell Res. 73, 103258 https://doi.org/10.1016/j.scr.2023.103258.

Klein, A., Lillis, S., Munteanu, I., Scoto, M., Zhou, H., Quinlivan, R., Straub, V., Manzur, A.Y., Roper, H., Jeannet, P.Y., Rakowicz, W., Jones, D.H., Jensen, U.B., Elizabethwraige, Trump, N., Schara, U., Lochmuller, H., Sarkozy, A., Kingston, H., Norwood, F., Damian, M., Kirschner, J., Longman, C., Roberts, M., Auer-Grumbach, M., Hughes, I., Bushby, K., Sewry, C., Robb, S., Abbs, S., Jungbluth, H., Muntoni, F., 2012. Clinical and genetic findings in a large cohort of patients with ryanodine receptor 1 gene-associated myopathies. Hum. Mutat. 33, 981–988. https://doi.org/10.1002/humu.22056.

Lorenzon, N.M., Beam, K.G., 2000. Calcium channelopathies. Kidney Int. 57, 794–802. https://doi.org/10.1046/j.1523-1755.2000.00917.x.

Monnier, N., Romero, N.B., Lerale, J., Landrieu, P., Nivoche, Y., Fardeau, M., Lunardi, J., 2001. Familial and sporadic forms of central core disease are associated with mutations in the C-terminal domain of the skeletal muscle ryanodine receptor. Hum. Mol. Genet. 10, 2581–2592. https://doi.org/10.1093/hmg/10.22.2581.

Quinlivan, R.M., Muller, C.R., Davis, M., Laing, N.G., Evans, G.A., Dwyer, J., Dove, J., Roberts, A.P., Sewry, C.A., 2003. Central core disease: clinical, pathological, and

genetic features. Arch. Dis. Child. 88, 1051–1055. https://doi.org/10.1136/adc.88.12.1051.

Samsó, M., 2017. A guide to the 3D structure of the ryanodine receptor type 1 by cryoEM. Protein Sci. 26, 52–68. https://doi.org/10.1002/pro.3052.

Treves, S., Anderson, A.A., Ducreux, S., Divet, A., Bleunven, C., Grasso, C., Paesante, S., Zorzato, F., 2005. Ryanodine receptor 1 mutations, dysregulation of calcium homeostasis and neuromuscular disorders. Neuromuscul. Disord. 15, 577–587. https://doi.org/10.1016/j.nmd.2005.06.008.

Wu, L., Brady, L., Shoffner, J., Tarnopolsky, M.A., 2018. Next-generation sequencing to diagnose Muscular dystrophy, rhabdomyolysis, and HyperCKemia. Can. J. Neurol. Sci. 45, 262–268. https://doi.org/10.1017/cjn.2017.286.

Wu, S., Ibarra, M.C.A., Malicdan, M.C.V., Murayama, K., Ichihara, Y., Kikuchi, H., Nonaka, I., Noguchi, S., Hayashi, Y.K., Nishino, I., 2006. Central core disease is due to RYR1 mutations in more than 90% of patients. Brain 129, 1470–1480. https://doi.org/10.1093/brain/awl077.

Zhang, H., Ma, Y., Lv, Y., Wan, Y., Zhao, Q., Gai, Z., Liu, Y., 2020. An integration-free iPSC line SDQLCHi025-a from a girl with multiminicore disease carrying compound heterozygote mutations in RYR1 gene. Stem Cell Res. 45, 101775 https://doi.org/10.1016/j.scr.2020.101775.